Zonal Characterization and Differential Trilineage Potentials of Equine Intrasynovial Deep Digital Flexor Tendon-Derived Cells

Vivian G Quam
The Ohio State University College of Veterinary Medicine
Nadine N Altmann
The Ohio State University College of Veterinary Medicine
Matthew T Brokken
The Ohio State University College of Veterinary Medicine
Sushmitha Durgam (durgam.3@osu.edu)
The Ohio State University https://orcid.org/0000-0002-5804-0406

Research article

Keywords: Intrasynovial deep digital flexor tendon, tendon-derived cells, trilineage differentiation, chondrogenic phenotype

Posted Date: December 4th, 2020

DOI: https://doi.org/10.21203/rs.3.rs-120378/v1

Version of Record: A version of this preprint was published at BMC Veterinary Research on April 1st, 2021.
See the published version at https://doi.org/10.1186/s12917-021-02793-1.

Abstract

Background: Intrasynovial deep digital flexor tendon (DDFT) injury is a common cause for forelimb lameness in horses and are typically associated with poor outcomes. Intrasynovial tendon contains a superficial fibrocartilage in response to compressive forces from an opposing boney prominence, and is critical for tendon gliding function. Characterization of tendon-derived cells (TDC) from intrasynovial tendon fibrocartilage has not been conducted as for prototypical extrasynovial tendon and is necessary for developing improved therapeutic strategies.

Results: In this study, we successfully isolated homogenous TDC from the fibrocartilaginous (fTDC) and tendinous (tTDC) zones of equine forelimb intrasynovial DDFT via low-density plating method. During monolayer passage, both TDC subpopulations exhibited clonogenicity, high in vitro proliferation rate, and fibroblast-like morphology. Third passage fTDC and tTDC were positive for cell surface antigens CD90 and CD29 and negative for CD44 and CD45. There were no significant differences in the basal tenogenic, osteogenic and chondrogenic marker expressions of fTDC and tTDC. Trilineage differentiation demonstrated that fTDC were largely restricted to chondrogenic differentiation; whereas, those from the tendinous zone underwent osteogenic and chondrogenic differentiation. Both TDC subpopulations displayed weak adipogenic differentiation potentials.

Conclusions: These results provide a foundation for studies exploring cell-based therapies for intrasynovial tendon repair as these TDC are potential targets to enhance intrinsic repair capacity. Pending further investigation, promoting chondrogenic properties in cells administered exogenously into the intrasynovial space may be beneficial for intrasynovial tendon regeneration.

Background

Deep digital flexor tendon (DDFT) injuries within the digital flexor tendon sheath (1, 2) and podotrochlear bursa (3–5) are common causes of forelimb lameness in horses. Therapeutic interventions such as surgical debridement of torn/fibrillated tendon fibers (2, 6), intrasynovial/local biologic or corticosteroid administration (3, 7), systemic NSAIDs (3, 8), and rehabilitation with activity restriction (3, 7, 8) are undertaken to optimize tendon healing and prevent long-term irreparable damage. While improper, fibrotic healing and repeat tendon tears or ruptures are common during extrasynovial and intrasynovial tendon healing; they are more frequent in intrasynovial tendons. Further, aforementioned therapies are also more efficacious for extrasynovial than intrasynovial tendon healing. Poor outcomes associated with intrasynovial DDFT injuries can be attributed, in part, to our minimal understanding of endogenous cellular processes specific to intrasynovial tendon and therefore, necessary for developing effective regenerative repair strategies.

Intrasynovial DDFT contains a superficial fibrocartilage at ‘wrap-around’ regions and where the tendon opposes boney prominences, which imparts a smooth surface and increased durability against abrasion (4, 5, 9). This fibrocartilaginous zone has been histologically described in human (10, 11), murine (12),

equine (5, 9, 13) and canine (14, 15) intrasynovial tendons and represents a functional adaptation to compressive loading from opposing boney prominence. Correspondingly, the extracellular matrix (ECM) within the tendon fibrocartilage is amorphous, rich in proteoglycans with 'rounded/chondrocyte-like' cells found within lacunae (9–12, 15). The fibrocartilaginous zone transitions to a tendinous zone composed of linear arrays of collagen fibers interspersed with spindle-shaped cells aligned along the longitudinal axis (9–12, 15). Cells within the fibrocartilaginous and tendinous zones function to maintain the structural heterogeneity of intrasynovial tendon ECM that provides compressive stiffness as well as tensile strength, respectively.

The cellular compartment of tendons, consisting of mature tenocytes and stem/progenitor cells, is small (< 1%), and is responsible for tendon ECM synthesis and turnover. Multipotent stem/progenitor cells have been characterized in tendons of several vertebrate species (16–19). In-vivo experimental studies have demonstrated that endogenous and exogenously administered tendon-derived cells (TDC) participate in tendon homeostasis and repair (16, 20–24). However, these studies are primarily focused on extrasynovial tendons. The purpose of this study was to isolate and systematically characterize TDC isolated from the fibrocartilaginous and tendinous zones of equine forelimb intrasynovial DDFT. Cells were isolated from tendon tissue within the proximal podotrochlear bursa and adjacent to the flexor surface of the distal sesamoid bone. First, we first investigated the colony formation, plasticity during monolayer passage and immunophenotype characteristics of the two TDC subpopulations. We then assessed the in vitro trilineage differentiation capacities of third passage TDC from the fibrocartilaginous (fTDC) and tendinous (tTDC) zones in relation to their respective terminally differentiated cells. Lastly, zonal variations in the aforementioned characteristics between fTDC and tTDC were evaluated.

Results

Morphology, clonogenicity and proliferation of intrasynovial TDC

At day 3 of culture, attached cells from the fibrocartilaginous zone exhibited polygonal morphology, and cells from the tendinous zone were elongate and spindle-shaped. By the third passage, both fTDC and tTDC were homogenous and exhibited fibroblast-like morphology (Fig. 1a).

The clonogenic capacity of intrasynovial TDC was determined using the colony forming unit (CFU) assay. The colonies from both fibrocartilaginous and tendinous zones were heterogenous in size and cell density (Fig. 1b). After 12–14 days, cells from the fibrocartilaginous and tendinous zones formed 28 ± 12 and 43 ± 9 colonies ($P = 0.12$), respectively from 1000 plated cells.

The time from initial plating of enzyme-digested fibrocartilaginous and tendinous zone cells to 70–80% confluence was 10.2 ± 1.2 days and 9.1 ± 1.6 days ($P = 0.6$), respectively. Population doubling time and population doublings during passage 1 and 2 were not significantly different between zones (Table 1).

Table 1
Population doubling (PD) and Population doubling time (PDT) of cells from the fibrocartilaginous and tendinous zones during first (P1) and second passages (P2) of monolayer expansion (mean ± SD days; n = 3).

	P1 PD	P1 PDT	P2 PD	P2 PDT
Fibrocartilaginous zone	1.6 ± 0.3	2.1 ± 1.2	1.8 ± 0.5	2.4 ± 1.1
Tendinous zone	1.8 ± 0.5	2.3 ± 0.9	1.9 ± 0.2	2.9 ± 1.6
p value	0.32	0.71	0.2	0.15

Phenotype characterization of fTDC and tTDC

Monolayer passage enriched for CD90, CD29 cells in both fTDC and tTDC; the cells expressed low levels of CD44 and were negative for hematopoietic marker, CD45 (Fig. 2). From the time of enzyme digestion to third passage, the percentage of $CD90^+$ cells increased from ~ 70% to 85–95%. Less than 5% of the cells were positive for CD44. The rates of $CD90^+$, $CD29^+$, $CD44^-$ and $CD45^-$ cells did not significantly differ between fTDC and tTDC.

Tenogenic (Fig. 3a), chondrogenic (Fig. 3b) and osteogenic mRNA of terminally differentiated cells, and fTDC and tTDC were assessed. Monolayer passage significantly down-regulated SCX (~ 10-fold) and COL1A1 (~ 3.5-fold) mRNA in fTDC and tTDC. There were no significant differences between the tenogenic mRNA expressions of fTDC and tTDC. SOX-9, COL2A1, ACAN and COL10A1 mRNA of fTDC and tTDC were significantly down-regulated relative to the respective terminally differentiated cells. In contrast, ALP mRNA of fTDC (5-fold; $P = 0.026$) and tTDC (2.8-fold; $P = 0.015$) was significantly increased. Similar to tenogenic mRNA, there were no significant differences between fTDC and tTDC chondrogenic mRNA. Osteogenic mRNA RUNX2 and SPARC were < 2-fold increased ($P > 0.05$) from respective terminally differentiated cells.

Chondrogenic Differentiation

Toluidine blue staining intensity of day 20 fTDC pellets was higher and uniformly distributed throughout the pellet demonstrating increasing sulfated glycosaminoglycan (sGAG) content compared to tTDC pellets (Fig. 4a). Correspondingly, sGAG quantity of day 20 fTDC chondrogenic pellets was significantly ($P = 0.02$) increased from tTDC pellets (Fig. 4b).

Chondrogenic stimulation significantly upregulated day 20 fTDC and tTDC pellets' SOX-9, ACAN and COL2A1 mRNA, compared to respective terminally differentiated cells (Fig. 4c). There were no significant differences between day 20 fTDC and tTDC values. Hypertrophic phenotype markers, ALP and COL10A1 were unaffected by chondrogenic stimulation.

Osteogenic Differentiation

Alizarin Red staining of day 21 osteogenic cultures demonstrated cell aggregation in both fTDC and tTDC; however mineralized matrix secretion was more evident in tTDC (Fig. 5a). Compared to day 0 cells,

alkaline phosphatase bioactivities (normalized to DNA content) of day 21 fTDC (5.6-fold; $P = 0.02$) and tTDC (6-fold; $P = 0.01$) cultures were significantly increased (Fig. 5b). Day 21 ALP bioactivities of fTDC and tTDC were not significantly different ($P = 0.07$).

Day 21 fTDC RUNX2, SPARC and ALP mRNA were not upregulated compared to terminally differentiated cells. In contrast, day 21 tTDC RUNX2 and ALP mRNA were significantly increased. Day 21 tTDC osteogenic mRNA was significantly higher than the corresponding fTDC values (Fig. 5c).

Adipogenic Differentiation

Day 14 Oil-Red-O stained adipogenic cultures showed cytoplasmic lipid droplet accumulation in both fTDC and tTDC, compared to day 0 cultures (Fig. 6a); however, stain uptake was minimal and the cells retained their fibroblast morphology. Dye elution and quantification (Fig. 6b) demonstrated 3 to 5.8-fold ($P = 0.03$) and 2 to 3.6-fold ($P = 0.02$) increase in fTDC and tTDC, respectively from day 0 cultures. Absorbance readings of day 14 fTDC adipogenic culture was 1.3 to 1.9-fold increased from tTDC ($P = 0.03$).

Discussion

Intrasynovial DDFT injury is a common source of debilitating forelimb lameness in horses. Chronic inflammation during healing and poor intrinsic healing potential are important factors responsible for dysregulated tissue repair. Tendon degeneration and adhesion formation within the synovial sheath are common sequelae that significantly reduce prognosis for return to function (3, 9, 13). Intrasynovial DDFT begins just proximal to the metacarpal(-tarsal) phalangeal (MCP/MTP) joint and extends to the distal second phalanx. Distally, the DDFT is compressed against the distal sesamoid bone within the podotrochlear bursa and surrounded by an annular pulley proximal to its insertion at the third phalanx (25). The dorsal fibrocartilage is robust at the level of MCP/MTP joint and proximal second phalanx and becomes thinner at the distal second phalanx, similar to rabbit (26), mouse (12) and canine (15, 27) DDFT. The large size, grossly distinct fibrocartilaginous-tendinous zones of the equine DDFT and ready access to healthy tissue facilitate cellular analyses described in this study. Intrasynovial TDC evaluated in this study were isolated using low-density plating method commonly used to isolate stem/progenitor cells from extrasynovial equine (18, 19, 28, 29), human (16), and mouse (16, 30) tendon tissues. We have designated these cells as TDC since further characterization is needed to determine if they possess stem/progenitor cell properties or if they are differentiated cells.

The clonogenic and monolayer passage characteristics of fTDC and tTDC were similar and consistent with existing extrasynovial tendon studies (16, 18, 19, 28). Freshly isolated primary cells following enzyme digestion of fibrocartilaginous and tendinous zones were heterogenous, with cells from the fibrocartilaginous zone exhibiting polygonal morphology and cells from the tendinous zone appearing elongate and spindle-shaped. However, after monolayer passage fTDC and tTDC became homogenous, fibroblast-like cells. The tenogenic and chondrogenic markers in fTDC and tTDC significantly decreased relative to their respective terminally differentiated cells and were not significantly different between

them. This plasticity property is seen in other tissue-derived stem/progenitor cells and highlights the key role of the ECM on their in-situ phenotype and bioactivities (16, 31, 32).

Cell surface marker profiles of equine intrasynovial TDC are comparable with extrasynovial tendon stem/progenitor cells (16, 33) and bone marrow-derived mesenchymal stem cells (18, 19, 28, 34). From the time of enzyme digestion to third passage, the percentage of $CD90^+$ cells increased from ~ 70% to 85–95%. While there were no differences in the cell surface markers of fTDC and tTDC, less than 5% of the cells were positive for CD44, a mesenchymal stromal cell marker. Further assessment of CD44 gene expression is warranted to determine if this is true to intrasynovial TDC, since an equine-specific antibody was utilized. Overall, it should be noted that our assessments of basal fTDC and tTDC phenotypes were restricted in this study, and a more robust analyses of cell surface markers and gene expression representing stem/progenitor cells such as CD73, CD105, Oct-4 are warranted.

Reflective of the in-situ chondrocyte-like morphology of tendon fibrocartilage cells, fTDC were largely restricted to chondrogenesis in vitro, whereas tTDC underwent osteogenic and chondrogenic differentiation. Although the basal (non-induced) osteogenic and chondrogenic mRNA profiles of fTDC and tTDC were not significantly different, basal fTDC SOX9 mRNA was 3-fold higher than tTDC and approached significance ($P = 0.06$; Fig. 4b). Subsequently, with chondrogenic stimulation, fTDC SOX-9 and ACAN mRNA expressions were 5- ($P = 0.07$) and 3.5- ($P = 0.06$) fold higher than tTDC. Toluidine blue stain uptake reflecting the sGAG content was also higher in fTDC pellets and was uniformly distributed throughout the pellet, whereas the stain uptake was just localized to the periphery of tTDC pellets (Fig. 4a). These findings suggest that fTDC may be ‘committed’ to a chondrogenic phenotype. However, additional analyses are required as it also possible that the low-density plating method selects for a chondrogenic fTDC subpopulation.

The common clonogenic, proliferative, and immunophenotype characteristics, and varying trilineage differentiation potentials of TDC isolated from morphologically distinct tendon zones are consistent in meniscal (35) and intervertebral disc (IVD) (36) tissues. In vitro chondrogenic restriction of stem/progenitor cells isolated from the inner zone of meniscus and IVD nucleus pulposus is partially implicated in the limited intrinsic repair capacity of these tissue zones. To this end, in-depth evaluation of cellular and healing responses of the fibrocartilage zone specifically during intrasynovial tendon injury is minimal. Nessler et al., evaluated healing in intrasynovial fibrocartilaginous and extrasynovial tendinous regions of canine DDFT after experimental longitudinal, partial thickness lacerations (15). The fibrocartilaginous region was stiffer and contained larger diameter collagen fibrils compared to tendinous regions at early timepoints during healing (3- and 6-weeks). This is reflective of local differential cellular synthetic activities and differences in mechanical environment during healing. Accepting that clinical tendon injuries require a prolonged time frame for recovery, longer-term in vivo experimental studies are warranted to delineate the mechanisms related to zonal differences in poor healing and re-rupture following intrasynovial injuries. Identifying these intrinsic cellular responses specific to intrasynovial tendon homeostasis, injury, and healing are critical to develop regenerative therapies aimed at restoring intrasynovial tendon gliding function.

The following factors pertaining to this study are to be taken into consideration. Intrasynovial TDC were isolated from healthy equine donors of a wide age range, albeit representative of age group susceptible to clinical disease (3–5, 9, 13, 37). Secondly, although low-density plating method is routinely used to isolate tendon stem/progenitor cells, alternate approaches such as differential substrate adherence or cell surface epitope FACS-based separation that mitigates monolayer passage and accelerates generation of relatively pure cell populations need to be evaluated. However, feasibility of these technologies when working with equine cell stocks is limited. Lastly, trilineage differentiation mRNA values in fTDC and tTDC were expressed as fold-change from respective (non-induced) terminally differentiated cells. Maintaining terminally differentiated subpopulations in basal medium for the same duration as induction media would have facilitated spontaneous differentiation assessments.

The collective outcomes of our data suggest presence of stem/progenitor cells in the fibrocartilaginous and tendinous zones of equine intrasynovial DDFT, and shares similarities with stem/progenitor cells characterized from equine extrasynovial superficial digital flexor tendon (18, 28). Consistent with Cadby *et al*., and Williamson *et al*., fTDC and tTDC expressed MSC properties such as clonogenicity and plasticity. These cells were also negative for hematopoietic stem cells markers (CD45, CD34), owing to poor tissue vascularity and supports that they were isolated from the tendon proper. In regard to trilineage differentiation, our results are similar to Williamson *et al*.; in that, adipogenic capacity was minimal (18). This is in contrast to Cadby *et al*., where cells underwent adipogenesis based on upregulated PPARg and FABP4 mRNA expression, as well as positive Oil-red O staining (28). tTDC exhibited osteogenic and chondrogenic capacities similar to stem/progenitor cells isolated from equine superficial digital flexor tendon as reported by Williamson *et al*. On the other hand, fTDC were largely restricted to chondrogenic differentiation, represents a unique TDC subpopulation and emphasizes the need for multi-assay panels for rigorous assessments of lineage commitment. While we have described fTDC characteristics in relation to their terminally differentiated cell counter parts and tTDC, comparative analyses with ‘gold standard’ bone marrow-derived mesenchymal stem cells could be more informative regarding their stem/progenitor cell characteristics.

The diminished healing capacity of intrasynovial tendons is attributed in part due to limited intrinsic healing mechanisms and inherent low tissue cellularity. The limitations in healing are also reflective of the mechanical environment within the tissue and persistent inflammation, consequently resulting in net tissue catabolism. The results of this study provide a foundation for studies evaluating cell-based therapies for intrasynovial tendon repair as these TDC are potential targets to enhance intrinsic repair. Promoting chondrogenic properties in cells administered exogenously into the intrasynovial space and in cells that are used to revitalize decellularized autografts may be beneficial for intrasynovial tendon regeneration. Future in vivo studies to evaluate the healing effects of intrasynovial TDC in experimental animal models are warranted.

Conclusions

This study investigated the characteristics of TDC isolated from the fibrocartilaginous and tendinous zones of the equine intrasynovial deep digital flexor tendon. Both TDC subpopulations exhibited clonogenicity and expressed similar cell surface antigen profiles. After 2 monolayer passages, chondrogenic and tenogenic markers were down-regulated in fTDC and tTDC indicative of plasticity property. There were no significant differences in the basal tenogenic, osteogenic and chondrogenic marker expressions of fTDC and tTDC. Trilineage differentiation demonstrated that fTDC were largely restricted to a chondrogenic lineage, whereas tTDC underwent both osteogenic and chondrogenic differentiation. Both fTDC and tTDC displayed weak adipogenic differentiation potentials. These results provide a foundation for studies exploring cell-based therapies for intrasynovial tendon repair as these TDC are potential targets to enhance intrinsic repair capacity.

Materials And Methods

Intrasynovial TDC isolation and culture

All procedures were approved by the University Institutional Animal Care and Use Committee. DDFTs were harvested from the forelimbs of five equine cadavers euthanized for reasons unrelated to musculoskeletal disorders (age range 6 to 12 years). Intrasynovial DDFT tissue within the proximal aspect of the podotrochlear bursa and adjacent to the distal sesamoid bone was used for TDC isolation and was determined free of gross pathology at the time of harvesting (9, 38). The dorsal fibrocartilaginous and underlying tendinous zones of DDFT were dissected by gross assessment (Fig. 7). From each horse about 1.5 and 3 grams of dorsal fibrocartilaginous and underlying tendinous tissues were obtained, respectively.

The tissue specimens were diced (0.25-cm^3) and cellular fractions isolated by dissociation in Dulbecco's modified Eagle's medium (DMEM; Gibco→, Carlsbad, CA) containing collagenase (Worthington, Lakewood, NJ) and supplemented with 2% fetal bovine serum (Gibco) and 1% penicillin-streptomycin (Gibco) at 37°C for 18 hours as previously described (16, 18, 19). Following optimization of tissue digestion; the fibrocartilaginous and tendinous zone tissues were digested with 0.15% collagenase type II and 0.2% collagenase type I, respectively. Primary cells from respective digests isolated by sequential filtration (40 microns) and centrifugation were seeded at 2,000 cells/cm^2 in monolayer cultures for expansion (18, 19, 30). At day 3 after primary culture, the unattached cells were removed by washing with PBS. Fresh culture medium was added every 3 days. Once discernable colonies (> 50 cells) were observed in both TDC subpopulations, they were detached using 0.05% trypsin-EDTA (Gibco) and sub-cultured. Subsequently, cells were detached at ~ 80% confluence and passaged twice. Third passage cells, designated as fTDC and tTDC here after were used for immunophenotyping and trilineage differentiation assays.

Colony-forming unit (CFU) assay and cell proliferation

Enzyme digested cells from fibrocartilaginous and tendinous zones were plated at 10 cells/cm^2 for colony forming unit (CFU) assay (16). After 14 days of culture, CFU assay was performed with 0.5% crystal violet staining after 4% paraformaldehyde fixation. All stained colonies (> 2 mm diameter) were counted.

Cell proliferation during first and second passages (P1 and P2) of TDC from both zones was calculated as population doublings using the formula: Log_2 (harvested cell number/seeded cell number). Population doubling times for TDC during passage 1 and 2 were calculated by dividing the time of each passage by the corresponding population doubling value (19).

Phenotype characterization of monolayer expanded TDC

Single-cell suspensions from TDC dissociated with 0.05% Trypsin-EDTA were used.

Flow cytometry and cell surface antigens

One million terminally differentiated cell from each zone, as well as fTDC and tTDC, were blocked with 10% BSA suspended in fluorescent activated cell sorting (FACS) buffer (pH 7.4 PBS with 1% BSA) for 20 minutes prior to washing. Cells were washed in PBS and resuspended in fluorescent conjugated or unconjugated primary antibodies and incubated at 4^0C for 30 minutes. The following antibodies were used according to the manufacturers' recommendations: anti-human conjugated anti-CD29-Alexa 488 (BioLegend, San Diego, CA); anti-horse conjugated anti-CD44-RPE (BioRad, Hercules, CA); anti-horse non-conjugated anti-CD90- conjugated with Alexa 647 (Accurate Chemicals, Westbury, NY) and anti-human conjugated anti-CD45-Alexa 488 (BioRad) (19). Cells were washed and resuspended in FACS buffer and analyzed by flow cytometry (Attune NxT Fluocytometer, ThermoFisher Sci, Waltham, MA). Cells blocked with 10% BSA and without antibody incubation or in the presence of secondary antibody alone were used as controls. A threshold gating out at least 95.5% of control cells was used. The percentage of positive cells was calculated and expressed as that exceeding the threshold.

Lineage-specific gene expression

Tenogenic, chondrogenic and osteogenic marker gene expressions were assessed in the respective terminally differentiated cells as well as fTDC and tTDC. Three million cells were stored for RNA isolation and quantitative real time-PCR (qRT-PCR) using SYBR Green Master Mix (Applied Biosystems, Foster City, CA), as detailed below for the following genes: scleraxis (SCX), tenomodulin (TNMD), collagen type I (COL1A1), collagen type III (COL3A1), cartilage oligomeric matrix protein (COMP); sex determining region Y-box9 (SOX-9), collagen type II (COL2A1), aggrecan (ACAN), alkaline phosphatase (ALP), collagen type X (COL10A1); runt-related transcription factor 2 (RUNX2) and osteonectin (SPARC).

Trilineage differentiation and phenotypic assays

Standard protocols for adipogenesis, osteogenesis and chondrogenesis assays were employed for trilineage differentiation assays of fTDC and tTDC, as described below (16, 18, 19).

Chondrogenic culture

Pellet cultures were established in microcentrifuge tubes from fTDC and tTDC by resuspending 5×10^5 cells/mL in chondrogenic medium (DMEM containing 100 U of sodium penicillin/mL and 100 µg of streptomycin sulfate/mL supplemented with 100 ηM dexamethasone, 25 µg/ml ascorbic acid, 10 ηg/ml TGF-β1, and 1% ITS media supplement), and pelleting 500 µl aliquots of the cell suspensions at 400 rcf for 8 minutes. Chondrogenic cultures were maintained for 20 days. Chondrogenic medium was replaced every 2 days.

Representative pellet sections were stained with toluidine blue to assess sGAG deposition after 20 days of chondrogenic culture. Cell pellets were fixed in 4% paraformaldehyde, dehydrated and embedded in paraffin. Six micron-thick sections were stained with toluidine blue prior to acquiring photomicrographs. Total sGAG within representative pellets (3 replicates each per horse) was measured using dimethyl methylene blue (DMMB) colorimetric assay.(39) Upregulation of chondrogenic genes SOX-9, COL2A1, ACAN, ALP and COL10A1 was assessed by qRT-PCR, as detailed below.

Osteogenic culture

fTDC and tTDC were plated at 10,000 cells/cm^2 in 6- and 12-well plates and cultured in complete DMEM until they reached 70–80% confluence. Complete DMEM was then substituted with osteogenic medium (DMEM containing 10% fetal bovine serum, 100 U of sodium penicillin/mL, and 100 µg of streptomycin sulfate/mL supplemented with 10 mM β glyceraldehyde-3-phosphate, 50 µg/mL ascorbic acid, 100 ηM dexamethasone). The medium was replaced every 2 days. The cultures were maintained for 21 days.

Alizarin Red staining was used to assess mineralized matrix deposition. The cell-matrix layer was washed with PBS and fixed with 70% ethanol and stained with 2% Alizarin Red stain for 10 min. Photomicrographs were obtained prior to osteogenic differentiation and at day 21 of osteogenic culture. Alkaline phosphatase bioactivity of representative cultures was measured (LabAssay ALP, Wako Chemicals, Richmond, VA) and normalized to the total DNA content (Quant-iT Pico Green kit, Life Technologies, Waltham, MA).(40) Upregulation of osteogenic transcription factor RUNX2 and osteoblast-specific proteins ALP and SPARC mRNA were assessed by qRT-PCR, as detailed below.

Adipogenic culture

fTDC and tTDC were plated at 5,000 cells/cm^2 in 12-well plates and cultured in complete DMEM until they reached 80% confluence. Complete DMEM was then substituted with adipogenic medium (DMEM containing 10% rabbit serum, 100 U of sodium penicillin/mL and 100 µg of streptomycin sulfate/mL and supplemented with 1 mM dexamethasone, 100 mM indomethacin, 10 mg/mL insulin, and 500 mM isobutylmethylxanthine). Medium was replaced every 2 days. These cultures were maintained for 14 days.

Oil-Red-O staining of cultures was used to detect intracellular lipid accumulation. Cell monolayers were washed with PBS, fixed with 70% ethanol for 30 minutes, and stained with 0.3% Oil-Red-O stain for 1 hour. Hematoxylin was added for 10 minutes. Photomicrographs were obtained prior to adipogenic

differentiation and at day 14 of adipogenic culture. Subsequently, Oil-Red-O stain was eluted with 2-propanol and absorbance of the eluate was spectrophotometrically quantified (Microplate Reader, Tecan Group Ltd, Switzerland) at 510 nm (41).

RNA isolation and qRT-PCR

Total RNA was isolated using a previously described protocol (19). The samples were homogenized in a guanidinium thiocyanate-phenol-chloroform solution reagent (TRIzol, ThermoFisher Scientific) according to manufacturer's suggested protocol. RNA isolation from the chondrogenic pellets included the high-salt precipitation variation, to minimize co-precipitation of proteoglycans. The resultant pellet was purified using RNeasy silica columns that included on-column DNase digestion. One μg of RNA from each sample was reverse-transcribed (Superscript IV, ThermoFisher Sci) using oligo(dT) primers. Equine gene-specific primers were designed from published sequences in Genbank and using ClustalW multiple sequence alignment (available at www.ebi.ac.uk) (Table 2). Primer specificity was confirmed by cloning and sequencing the amplicons during optimization experiments, as previously described (19, 24, 42). PCR amplifications were catalyzed by Taq DNA polymerase (QuantStudio 3, Applied Biosystems, ThermoFisher Sci) in the presence of Sybr Green. Relative gene expression was quantified using the $2^{-\Delta\Delta CT}$ method, normalized to expression of the reference gene, elongation factor-1α (EF1α) (43).

Table 2
Primer sequences used for qRT-PCR.

Gene		Sequence	Amplicon (bp)
SCX	S	5’ GAC CGC ACC AAC AGT GTG AA	231
	A	5’ TGG TTG CTG AGG CAG AAG GT	
COL1A1	S	5’ GAA AAC ATC CCA GCC AAG AA	231
	A	5’ GAT TGC CAG TCT CCT CAT CC	
COL3A1	S	5’ AGG GGA CCT GGT TAC TGC TT	215
	A	5’ TCT CTG GGT TGG GAC AGT CT	
COMP	S	5’ TCA TGT GGA AGC AGA TGG AG	223
	A	5’ TAG GAA CCA GCG GTA GGA TG	
RUNX2	S	5’ CAG ACC AGC AGC ACT CCA TA	177
	A	5’ CAG CGT CAA CAC CAT CAT TC	
SPARC	S	5’ AAC CTT CTG ACC GAG AAG CA	190
	A	5’ TGG GAC AGG TAC CCA TCA AT	
ALP	S	5’ TGG GGT GAA GGC TAA TGA GG	221
	A	5’ GGC ATC TCG TTG TCC GAG TA	
SOX-9	S	5’ GAA CGC ACA TCA AGA CGG AG	304
	A	5’ CTG GTG GTC TGT GTA GTC GT	
COL2A1	S	5’ AGC AGG AAT TTG GTG TGG AC	223
	A	5’ TCT GCC CAG TTC AGG TCT CT	
ACAN	S	5’ GAC GCC GAG AGC AGG TGT	202
	A	5’ AAG AAG TTG TCG GGC TGG TT	
COL10A1	S	5’ TGC CAA CCA GGG TGT AAC AG	244
	A	5’ ACA TTA CTG GGG TGC CGT TC	
EF1α	S	5’ CCC GGA CAC AGA GAC TTC AT	328
	A	5’ AGC ATG TTG TCA CCA TTC CA	

Statistical analysis

Normal distribution of quantitative data was assessed using the Kolmogorov-Smirnov test. Data are expressed as mean ± standard deviation or as median and interquartile ranges. Comparative differences between cells from fibrocartilaginous and tendinous zones were analyzed for CFU and cell proliferation. Plasticity during monolayer passage with respect to cell surface antigens and tenogenic, osteogenic and chondrogenic marker gene expressions (between terminally differentiated cells and, fTDC and tTDC) was evaluated. Subsequently, trilineage differentiation potentials of fTDC and tTDC were assessed via fold change in gene expression of end-point induction cultures from respective terminally differentiated cells. One-way analysis of variance (ANOVA) or its non-parametric equivalent, Kruskal Wallis test was used to analyze and compare results within and between cells from fibrocartilaginous and tendinous zones. All analyses were conducted using SigmaStat 4 software (Systat Software, San Jose, CA). Significance was set at $P \leq 0.05$.

Abbreviations

DDFT: Deep digital flexor tendon; ECM: Extracellular matrix; TDC: Tendon-derived cells; fTDC: TDC from fibrocartilaginous zone; tTDC: TDC from tendinous zone; CFU: Colony forming unit; FACS: fluorescent activated cell sorting; SCX: Scleraxis; COL1A1: Collagen type I; SOX-9: Sex determining region Y-box 9; COL2A1: Collagen type II; COL3A1: Collagen type III; COMP: Cartilage oligomeric matrix protein; ACAN: Aggrecan; COL10A1: Collagen type X; ALP: Alkaline phosphatase; RUNX2: Runt-related transcription factor 2; SPARC: Osteonectin; EF1a: Elongation factor-1a; sGAG: sulfated glycosaminoglycan; DMEM: Dulbecco's modified Eagle's medium; PBS: Phosphate buffered saline; DMMB: Dimethyl methylene blue; qRT-PCR: quantitative real time polymerase chain reaction; ANOVA: Analysis of variance

Declarations

Ethics approval and consent to participate: The tendon samples utilized in this study were obtained from horses that were donated to the university for research purposes following euthanasia. As such, an ethical review process specific to this study was not required.

Consent for publication: Not applicable

Availability of data and materials: The data sets supporting the results of this manuscript will be made available by the authors, without any reservation, to researchers upon request.

Competing interests: The authors declare that the research was conducted in the absence of any commercial or financial relationships that could be construed as a potential conflict of interest.

Funding: Funding was obtained from The Ohio State University Equine Research Fund by the Ohio State Racing Commission. The funding agency was not involved in the design, analysis and reporting of the study.

Authors' contributions: VQ and SD obtained funding for the study, conducted experiments, and analysed the data. NA contributed to the acquisition, analysis and interpreted the data. SD conceived the study design. All authors wrote, critically revised the manuscript for intellectual content; and approved the final submitted version of the manuscript.

Acknowledgements: We would like to thank Dr. Matthew Stewart for professional advice on manuscript preparation.

Authors' information (optional): As detailed in title page.

References

1. Barr AR, Dyson SJ, Barr FJ, O'Brien JK. Tendonitis of the deep digital flexor tendon in the distal metacarpal/metatarsal region associated with tenosynovitis of the digital sheath in the horse. Equine Vet J. 1995 Sep;27(5):348–55. PubMed PMID: 8654349. eng.
2. Arensburg L, Wilderjans H, Simon O, Dewulf J, Boussauw B. Nonseptic tenosynovitis of the digital flexor tendon sheath caused by longitudinal tears in the digital flexor tendons: a retrospective study of 135 tenoscopic procedures. Equine Vet J. 2011 Nov;43(6):660–8. PubMed PMID: 21649711. Epub 2011/06/08. eng.
3. Lutter JD, Schneider RK, Sampson SN, Cary JA, Roberts GD, Vahl CI. Medical treatment of horses with deep digital flexor tendon injuries diagnosed with high-field-strength magnetic resonance imaging: 118 cases (2000–2010). J Am Vet Med Assoc. 2015 Dec;247(11):1309–18. PubMed PMID: 26594815. eng.
4. Blunden A, Dyson S, Murray R, Schramme M. Histopathology in horses with chronic palmar foot pain and age-matched controls. Part 1: Navicular bone and related structures. Equine Vet J. 2006 Jan;38(1):15–22. PubMed PMID: 16411581. Epub 2006/01/18. eng.
5. Blunden A, Murray R, Dyson S. Lesions of the deep digital flexor tendon in the digit: a correlative MRI and post mortem study in control and lame horses. Equine Vet J. 2009 Jan;41(1):25–33. PubMed PMID: 19301578. Epub 2009/03/24. eng.
6. Smith MR, Wright IM. Endoscopic evaluation of the navicular bursa: observations, treatment and outcome in 92 cases with identified pathology. Equine Vet J. 2012 May;44(3):339–45. PubMed PMID: 21848532. Epub 2011/08/18. eng.
7. Marsh CA, Schneider RK, Sampson SN, Roberts GD. Response to injection of the navicular bursa with corticosteroid and hyaluronan following high-field magnetic resonance imaging in horses with signs of navicular syndrome: 101 cases (2000–2008). J Am Vet Med Assoc. 2012 Nov;241(10):1353–64. PubMed PMID: 23113529. eng.
8. Gutierrez-Nibeyro SD, White Ii NA, Werpy NM. Outcome of medical treatment for horses with foot pain: 56 cases. Equine Vet J. 2010 Nov;42(8):680–5. PubMed PMID: 21039796. Epub 2010/08/19. eng.

9. Beck S, Blunden T, Dyson S, Murray R. Are matrix and vascular changes involved in the pathogenesis of deep digital flexor tendon injury in the horse? Vet J. 2011 Sep;189(3):289–95. PubMed PMID: 21821448. Epub 2011/08/09. eng.
10. Benjamin M, Qin S, Ralphs JR. Fibrocartilage associated with human tendons and their pulleys. J Anat. 1995 Dec;187 (Pt 3):625 – 33. PubMed PMID: 8586561. PMCID: PMC1167465. eng.
11. Benjamin M, Ralphs JR. Fibrocartilage in tendons and ligaments–an adaptation to compressive load. J Anat. 1998 Nov;193 (Pt 4):481 – 94. PubMed PMID: 10029181. PMCID: PMC1467873. eng.
12. Wong J, Bennett W, Ferguson MW, McGrouther DA. Microscopic and histological examination of the mouse hindpaw digit and flexor tendon arrangement with 3D reconstruction. J Anat. 2006 Oct;209(4):533–45. PubMed PMID: 17005025. PMCID: PMC2100351. eng.
13. Blunden A, Dyson S, Murray R, Schramme M. Histopathology in horses with chronic palmar foot pain and age-matched controls. Part 2: The deep digital flexor tendon. Equine Vet J. 2006 Jan;38(1):23–7. PubMed PMID: 16411582. Epub 2006/01/18. eng.
14. Bi C, Thoreson AR, Zhao C. The effects of lyophilization on flexural stiffness of extrasynovial and intrasynovial tendon. J Biomech. 2018 07;76:229 – 34. PubMed PMID: 29935733. Epub 2018/06/18. eng.
15. Nessler JP, Amadio PC, Berglund LJ, An KN. Healing of canine tendon in zones subjected to different mechanical forces. J Hand Surg Br. 1992 Oct;17(5):561–8. PubMed PMID: 1479251. eng.
16. Bi Y, Ehirchiou D, Kilts TM, Inkson CA, Embree MC, Sonoyama W, et al. Identification of tendon stem/progenitor cells and the role of the extracellular matrix in their niche. Nat Med. 2007 Oct;13(10):1219–27. PubMed PMID: 17828274. Epub 2007/09/09. eng.
17. Rui YF, Lui PP, Li G, Fu SC, Lee YW, Chan KM. Isolation and characterization of multipotent rat tendon-derived stem cells. Tissue Eng Part A. 2010 May;16(5):1549–58. PubMed PMID: 20001227. eng.
18. Williamson KA, Lee KJ, Humphreys WJ, Comerford EJ, Clegg PD, Canty-Laird EG. Restricted differentiation potential of progenitor cell populations obtained from the equine superficial digital flexor tendon (SDFT). J Orthop Res. 2015 Jun;33(6):849–58. PubMed PMID: 25877997. PMCID: PMC4657492. eng.
19. Durgam S, Schuster B, Cymerman A, Stewart A, Stewart M. Differential Adhesion Selection for Enrichment of Tendon-Derived Progenitor Cells During In Vitro Culture. Tissue Eng Part C Methods. 2016;08(8):801–8. 22(. PubMed PMID: 27406327. Epub 2016/08/01. eng.
20. Lee CH, Lee FY, Tarafder S, Kao K, Jun Y, Yang G, et al. Harnessing endogenous stem/progenitor cells for tendon regeneration. J Clin Invest. 2015 Jul 1;125(7):2690 – 701. PubMed PMID: 26053662. PMCID: PMC4563693. Epub 2015/06/09. eng.
21. Tarafder S, Brito JA, Minhas S, Effiong L, Thomopoulos S, Lee CH. In situ tissue engineering of the tendon-to-bone interface by endogenous stem/progenitor cells. Biofabrication. 2019 Nov 18;12(1):015008. PubMed PMID: 31561236. PMCID: PMC6904927. Epub 2019/09/29. eng.

22. Sakabe T, Sakai K, Maeda T, Sunaga A, Furuta N, Schweitzer R, et al. Transcription factor scleraxis vitally contributes to progenitor lineage direction in wound healing of adult tendon in mice. J Biol Chem. 2018 Apr 20;293(16):5766-80. PubMed PMID: 29507095. PMCID: PMC5912447. Epub 2018/03/07. eng.
23. Runesson E, Ackermann P, Karlsson J, Eriksson BI. Nucleostemin- and Oct 3/4-positive stem/progenitor cells exhibit disparate anatomical and temporal expression during rat Achilles tendon healing. BMC Musculoskelet Disord. 2015 Aug 20;16:212. PubMed PMID: 26290425. PMCID: PMC4545962. Epub 2015/08/21. eng.
24. Durgam SS, Stewart AA, Sivaguru M, Wagoner Johnson AJ, Stewart MC. Tendon-derived progenitor cells improve healing of collagenase-induced flexor tendinitis. J Orthop Res. 2016 12;34(12):2162-71. PubMed PMID: 27035120. Epub 2016/04/07. eng.
25. Denoix J-M. The Equine Distal Limb: CRC Press: Taylor & Francis Group; 2014.
26. Giori NJ, Beaupre GS, Carter DR. Cellular shape and pressure may mediate mechanical control of tissue composition in tendons. J Orthop Res. 1993 Jul;11(4):581–91.
27. Kadar A, Thoreson AR, Reisdorf RL, Amadio PC, Moran SL, Zhao C. Turkey model for flexor tendon research: in vitro comparison of human, canine, turkey, and chicken tendons. J Surg Res. 2017 08;216:46–55. PubMed PMID: 28807213. Epub 2017/04/01. eng.
28. Cadby JA, Buehler E, Godbout C, van Weeren PR, Snedeker JG. Differences between the cell populations from the peritenon and the tendon core with regard to their potential implication in tendon repair. PLoS One. 2014;9(3):e92474. PubMed PMID: 24651449. PMCID: PMC3961373. Epub 2014/03/20. eng.
29. Lovati AB, Corradetti B, Lange Consiglio A, Recordati C, Bonacina E, Bizzaro D, et al. Characterization and differentiation of equine tendon-derived progenitor cells. J Biol Regul Homeost Agents. 2011 2011 Apr-Jun;25(2 Suppl):S75-84. PubMed PMID: 22051173. eng.
30. Asai S, Otsuru S, Candela ME, Cantley L, Uchibe K, Hofmann TJ, et al. Tendon progenitor cells in injured tendons have strong chondrogenic potential: the CD105-negative subpopulation induces chondrogenic degeneration. Stem Cells. 2014 Dec;32(12):3266–77. PubMed PMID: 25220576. PMCID: PMC4245375. eng.
31. Clements LE, Garvican ER, Dudhia J, Smith RK. Modulation of mesenchymal stem cell genotype and phenotype by extracellular matrix proteins. Connect Tissue Res. 2016 11;57(6):443 – 53. PubMed PMID: 27448620. Epub 2016/07/22. eng.
32. McCorry MC, Puetzer JL, Bonassar LJ. Characterization of mesenchymal stem cells and fibrochondrocytes in three-dimensional co-culture: analysis of cell shape, matrix production, and mechanical performance. Stem Cell Res Ther. 2016 Mar;7:39. PubMed PMID: 26971202. PMCID: PMC4789279. Epub 2016/03/12. eng.
33. Tan Q, Lui PP, Rui YF. Effect of in vitro passaging on the stem cell-related properties of tendon-derived stem cells-implications in tissue engineering. Stem Cells Dev. 2012 Mar;21(5):790–800. PubMed PMID: 21627568. PMCID: PMC3295857. Epub 2011/08/08. eng.

34. De Schauwer C, Piepers S, Van de Walle GR, Demeyere K, Hoogewijs MK, Govaere JL, et al. In search for cross-reactivity to immunophenotype equine mesenchymal stromal cells by multicolor flow cytometry. Cytometry A. 2012 Apr;81(4):312–23. PubMed PMID: 22411893. Epub 2012/03/12. eng.
35. Mauck RL, Martinez-Diaz GJ, Yuan X, Tuan RS. Regional multilineage differentiation potential of meniscal fibrochondrocytes: implications for meniscus repair. Anat Rec (Hoboken). 2007 Jan;290(1):48–58. PubMed PMID: 17441197. eng.
36. De Luca P, Castagnetta M, de Girolamo L, Coco S, Malacarne M, Ragni E, et al. Intervertebral disc and endplate cell characterisation highlights annulus fibrosus cells as the most promising for tissue-specific disc degeneration therapy. Eur Cell Mater. 2020 Mar;39:156–70. PubMed PMID: 32125689. Epub 2020/03/03. eng.
37. Murray RC, Schramme MC, Dyson SJ, Branch MV, Blunden TS. Magnetic resonance imaging characteristics of the foot in horses with palmar foot pain and control horses. Vet Radiol Ultrasound. 2006 Jan-Feb;47(1):1–16. PubMed PMID: 16429980. Epub 2006/01/25. eng.
38. Sullivan SN, Cole SC, Stewart MC, Brokken MT, Durgam SS. Ex vivo effects of corticosteroids on equine deep digital flexor and navicular fibrocartilage cell viability. Am J Vet Res (accepted for publication).
39. Zheng CH, Levenston ME. Fact versus artifact: avoiding erroneous estimates of sulfated glycosaminoglycan content using the dimethylmethylene blue colorimetric assay for tissue-engineered constructs. Eur Cell Mater. 2015 Apr;29:224 – 36; discussion 36. PubMed PMID: 25890595. PMCID: PMC4445729. Epub 2015/04/19. eng.
40. Kyllönen L, Haimi S, Mannerström B, Huhtala H, Rajala KM, Skottman H, et al. Effects of different serum conditions on osteogenic differentiation of human adipose stem cells in vitro. Stem Cell Res Ther. 2013 Feb;4(1):17. PubMed PMID: 23415114. PMCID: PMC3706769. Epub 2013/02/15. eng.
41. Kraus NA, Ehebauer F, Zapp B, Rudolphi B, Kraus BJ, Kraus D. Quantitative assessment of adipocyte differentiation in cell culture. Adipocyte. 2016 2016 Oct-Dec;5(4):351–8. PubMed PMID: 27994948. PMCID: PMC5160397. Epub 2016/09/26. eng.
42. Durgam SS, Altmann NN, Coughlin HE, Rollins A, Hostnik LD. Insulin Enhances the In Vitro Osteogenic Capacity of Flexor Tendon-Derived Progenitor Cells. Stem Cells Int. 2019;2019:1602751. PubMed PMID: 31949435. PMCID: PMC6948345. Epub 2019/12/27. eng.
43. Livak KJ, Schmittgen TD. Analysis of relative gene expression data using real-time quantitative PCR and the 2(-Delta Delta C(T)) Method. Methods. 2001 Dec;25(4):402–8. PubMed PMID: 11846609. eng.

Figures

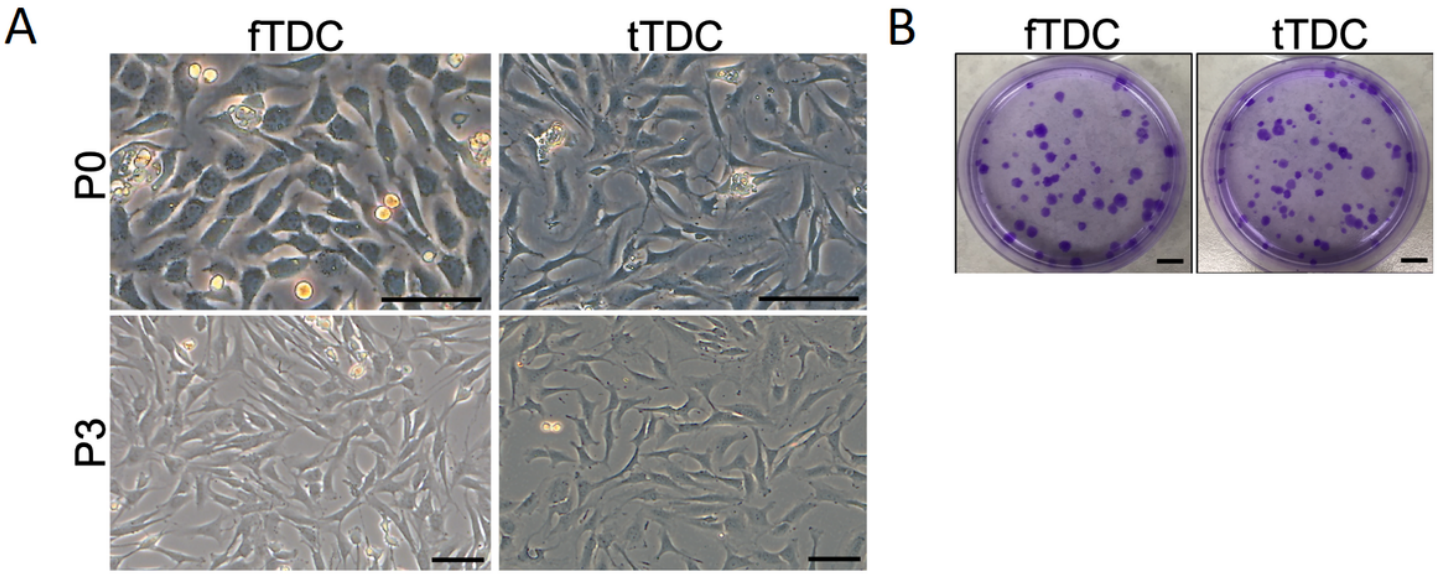

Figure 1

Equine intrasynovial TDC in vitro morphology and CFU (a) Morphology of TDC during monolayer passage. At passage 0 (P0), attached cells from the fibrocartilaginous and tendinous zones were polygonal and elongate/spindle-shaped cells, respectively. At passage 3 (P3), both fTDC and tTDC were homogenous and exhibited fibroblast-like morphology. Scale bar = 100 microns. (b) Colony forming unit assay of cells from the fibrocartilaginous and tendinous zones after 10 days of culture. Scale bar = 1 cm.

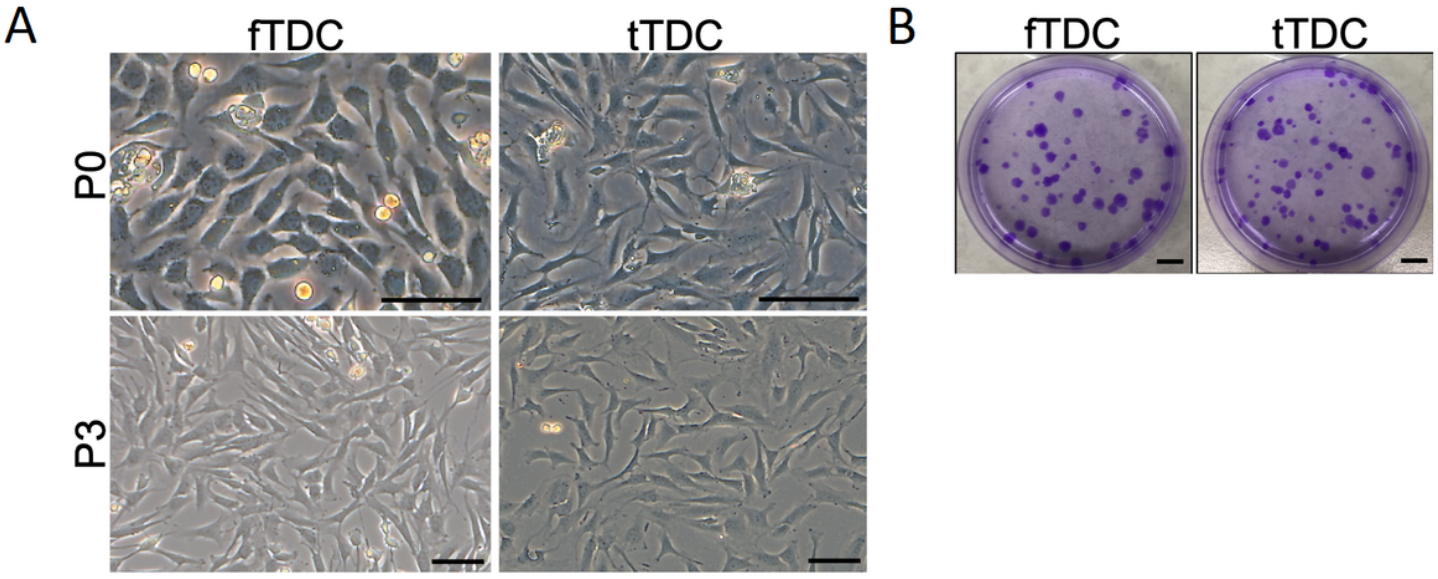

Figure 1

Equine intrasynovial TDC in vitro morphology and CFU (a) Morphology of TDC during monolayer passage. At passage 0 (P0), attached cells from the fibrocartilaginous and tendinous zones were polygonal and elongate/spindle-shaped cells, respectively. At passage 3 (P3), both fTDC and tTDC were

homogenous and exhibited fibroblast-like morphology. Scale bar = 100 microns. (b) Colony forming unit assay of cells from the fibrocartilaginous and tendinous zones after 10 days of culture. Scale bar = 1 cm.

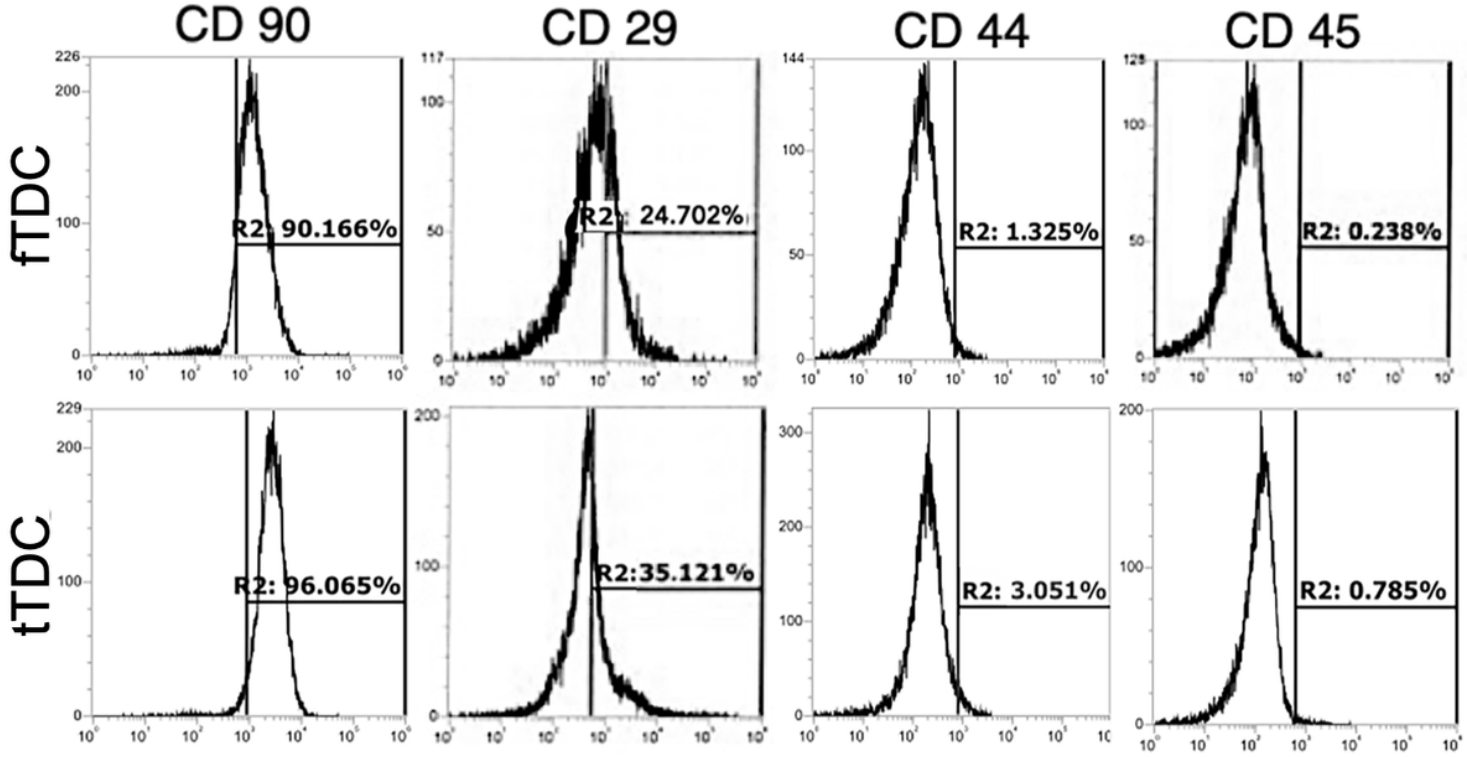

Figure 2

Equine intrasynovial TDC immunophenotype. Representative fluorescent activated cell sorting (FACS) analysis of cell surface markers CD90, CD29, CD44 and CD45 of fTDC and tTDC. n = 3.

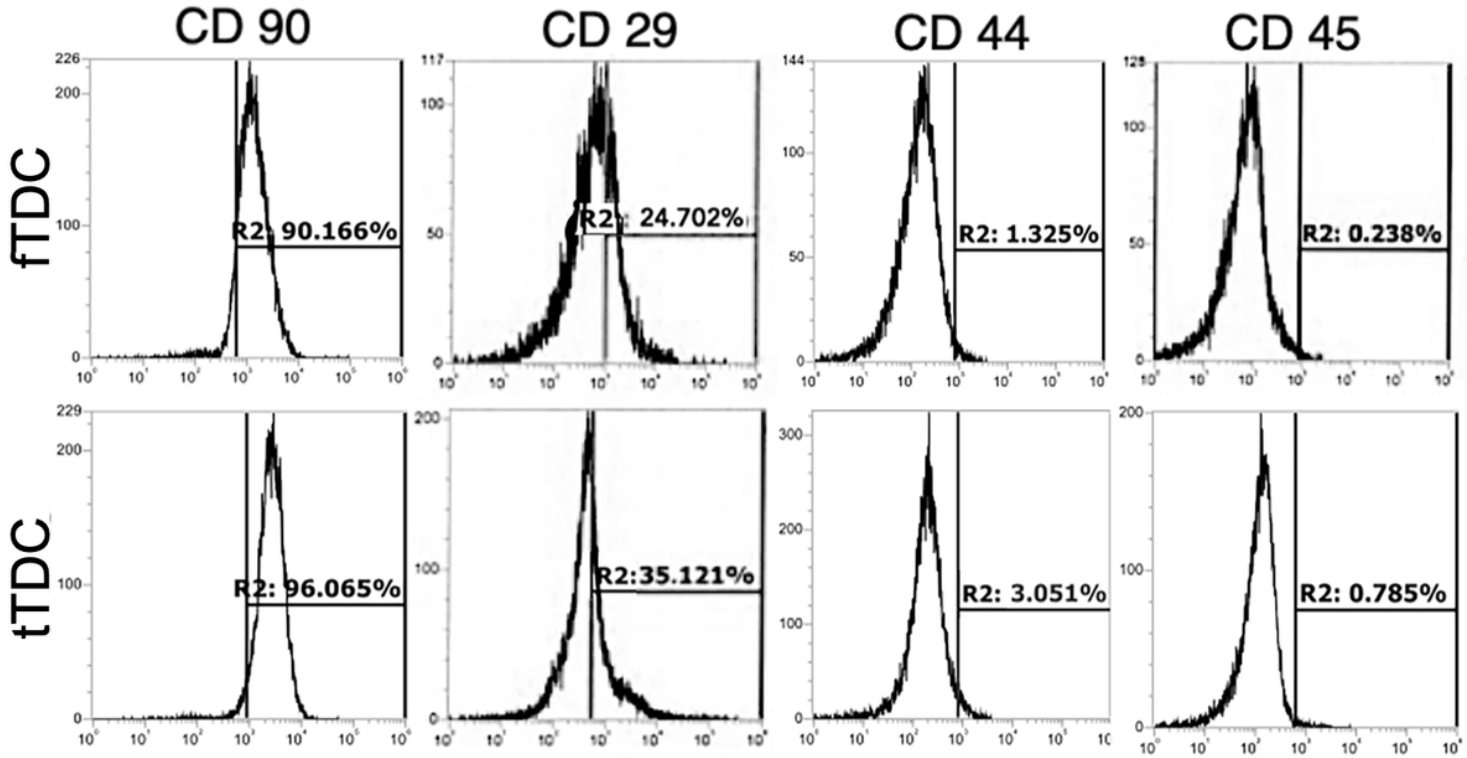

Figure 2

Equine intrasynovial TDC immunophenotype. Representative fluorescent activated cell sorting (FACS) analysis of cell surface markers CD90, CD29, CD44 and CD45 of fTDC and tTDC. n = 3.

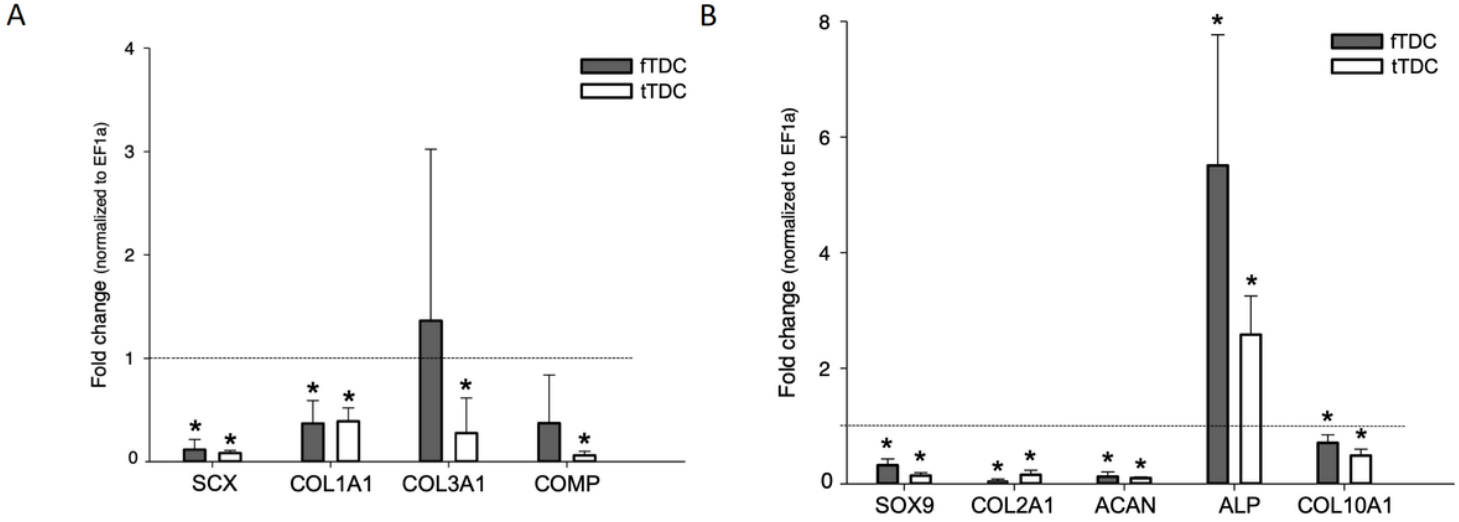

Figure 3

Equine intrasynovial TDC gene expression. (a) Tenogenic and (b) Chondrogenic gene expressions of fTDC and tTDC. Bars represent mean + SD of relative gene expression compared to respective terminally differentiated cells (dotted line) and normalized to EF1. * represents significant difference (P < 0.05) from respective terminally differentiated cells. n = 3.

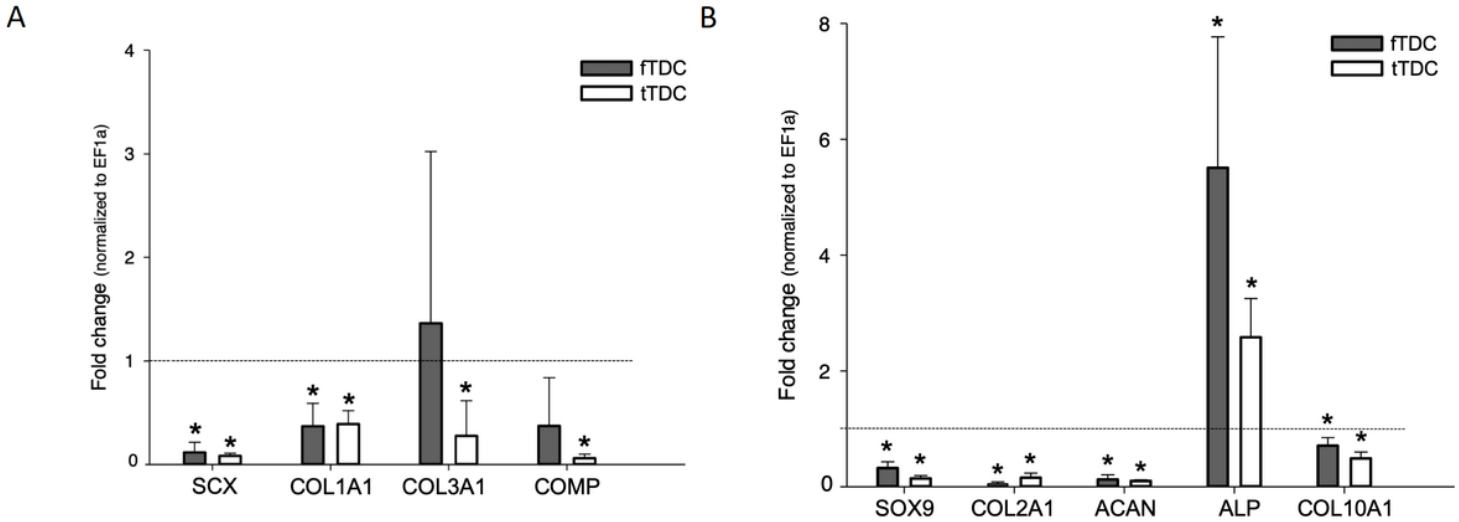

Figure 3

Equine intrasynovial TDC gene expression. (a) Tenogenic and (b) Chondrogenic gene expressions of fTDC and tTDC. Bars represent mean + SD of relative gene expression compared to respective terminally differentiated cells (dotted line) and normalized to EF1. * represents significant difference (P < 0.05) from respective terminally differentiated cells. n = 3.

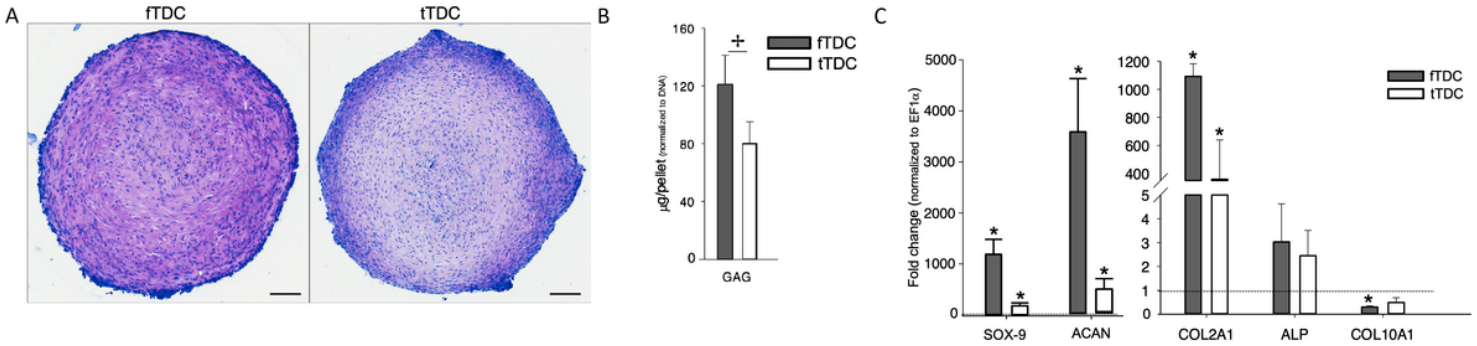

Figure 4

Chondrogenesis of fTDC and tTDC. (a) Toluidine blue staining of day 20 chondrogenic pellets. Stain uptake and metachromatic hue reflective of sGAG content are higher in fTDC pellets. Scale bar = 100 microns. (b) sGAG contents of day 20 fTDC and tTDC pellets normalized to DNA content. (c) Chondrogenic gene expression. Box-whisker plots represent medians and inter-quartile ranges (SOX-9 and ACAN), and bars represent mean + SD (COL2A1, ALP, COL10A1) relative to terminally differentiated cells (dotted line) and normalized to EF1□. * represents significant difference ($p < 0.05$) from respective terminally differentiated cells. □ represents significant difference ($p < 0.05$) between day 21 fTDC and tTDC. n = 5.

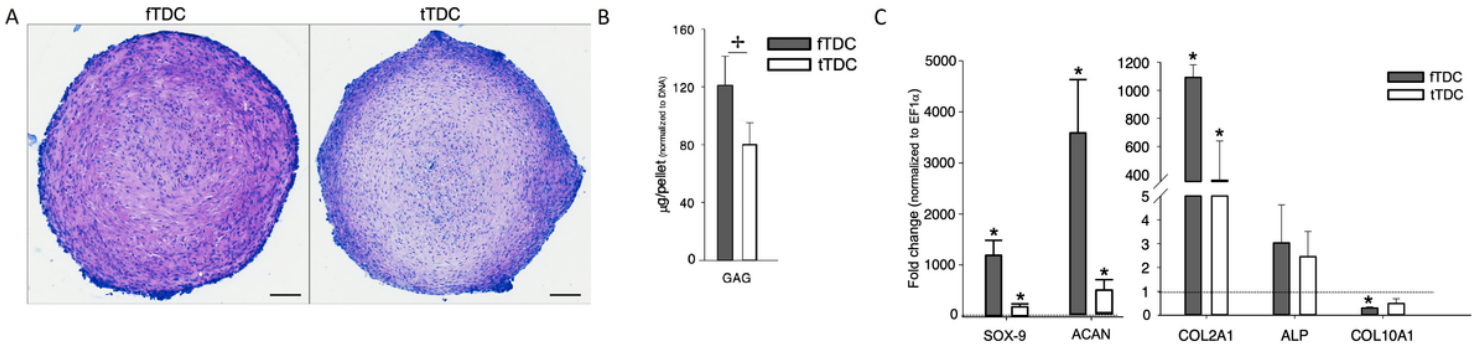

Figure 4

Chondrogenesis of fTDC and tTDC. (a) Toluidine blue staining of day 20 chondrogenic pellets. Stain uptake and metachromatic hue reflective of sGAG content are higher in fTDC pellets. Scale bar = 100 microns. (b) sGAG contents of day 20 fTDC and tTDC pellets normalized to DNA content. (c) Chondrogenic gene expression. Box-whisker plots represent medians and inter-quartile ranges (SOX-9 and ACAN), and bars represent mean + SD (COL2A1, ALP, COL10A1) relative to terminally differentiated cells (dotted line) and normalized to EF1□. * represents significant difference ($p < 0.05$) from respective terminally differentiated cells. □ represents significant difference ($p < 0.05$) between day 21 fTDC and tTDC. n = 5.

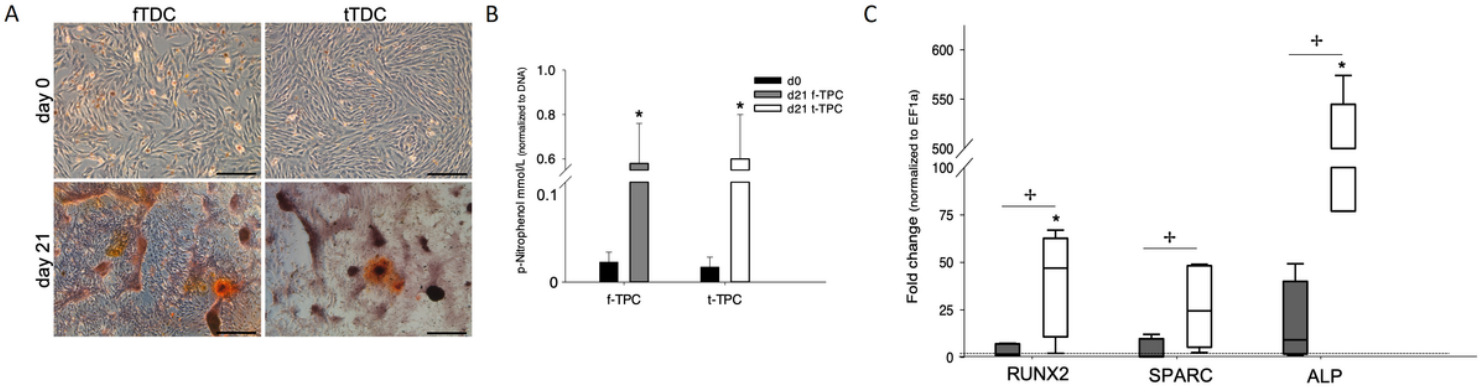

Figure 5

Osteogenesis of fTDC and tTDC. (a) Alizarin Red staining of day 0 and 21 osteogenic cultures. Cell aggregation and mineralized matrix secretion are more apparent in tTDC. Scale bar = 100 microns. (b) Alkaline phosphatase bioactivities of day 0 and 21 fTDC and tTDC osteogenic cultures normalized to DNA content. (c) Osteogenic gene expression. Box-whisker plots represent medians and inter-quartile ranges relative to terminally differentiated cells (dotted line) and normalized to EF1α. * represents significant difference ($P < 0.05$) from respective terminally differentiated cells. + represents significant difference ($P < 0.05$) between day 21 fTDC and tTDC. n = 5.

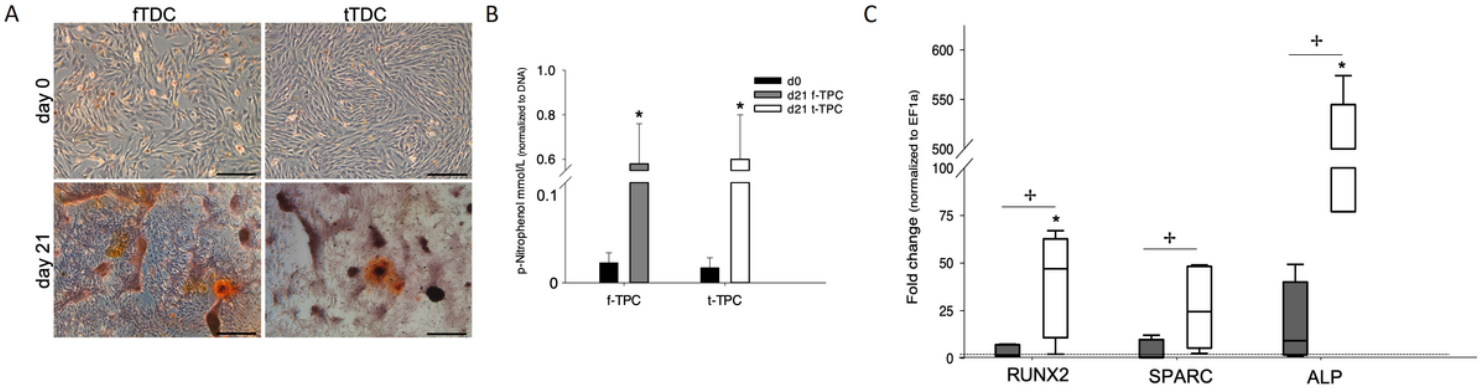

Figure 5

Osteogenesis of fTDC and tTDC. (a) Alizarin Red staining of day 0 and 21 osteogenic cultures. Cell aggregation and mineralized matrix secretion are more apparent in tTDC. Scale bar = 100 microns. (b) Alkaline phosphatase bioactivities of day 0 and 21 fTDC and tTDC osteogenic cultures normalized to DNA content. (c) Osteogenic gene expression. Box-whisker plots represent medians and inter-quartile ranges relative to terminally differentiated cells (dotted line) and normalized to EF1α. * represents significant difference ($P < 0.05$) from respective terminally differentiated cells. + represents significant difference ($P < 0.05$) between day 21 fTDC and tTDC. n = 5.

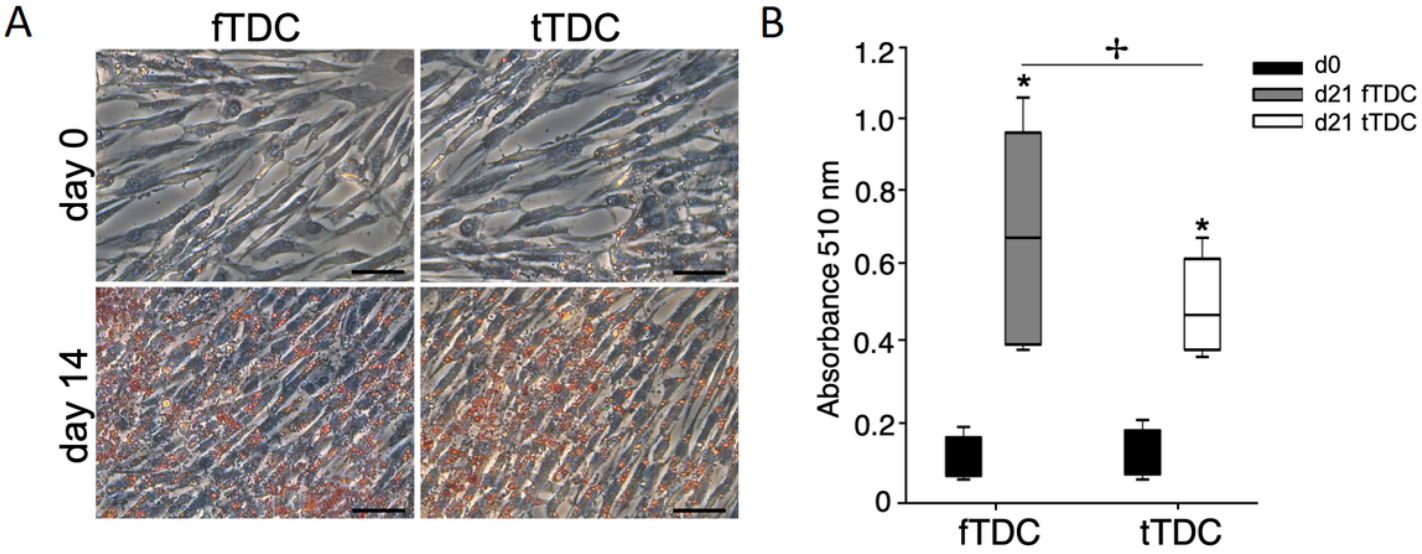

Figure 6

Adipogenesis of fTDC and tTDC. (a) Oil-Red-O staining of day 0 and 14 adipogenic cultures. Cytoplasmic lipid droplets were present in day 14 fTDC and tTDC; however, the cells retained their fibroblast morphology. Scale bar = 100 microns (b) Absorbance readings (mean + SD) following dye elution of Oil-Red-O stained day 0 and 14 cultures. * represents significant difference ($P < 0.05$) from day 0 cultures. represents significant difference ($P < 0.05$) between day 14 fTDC and tTDC. n = 3.

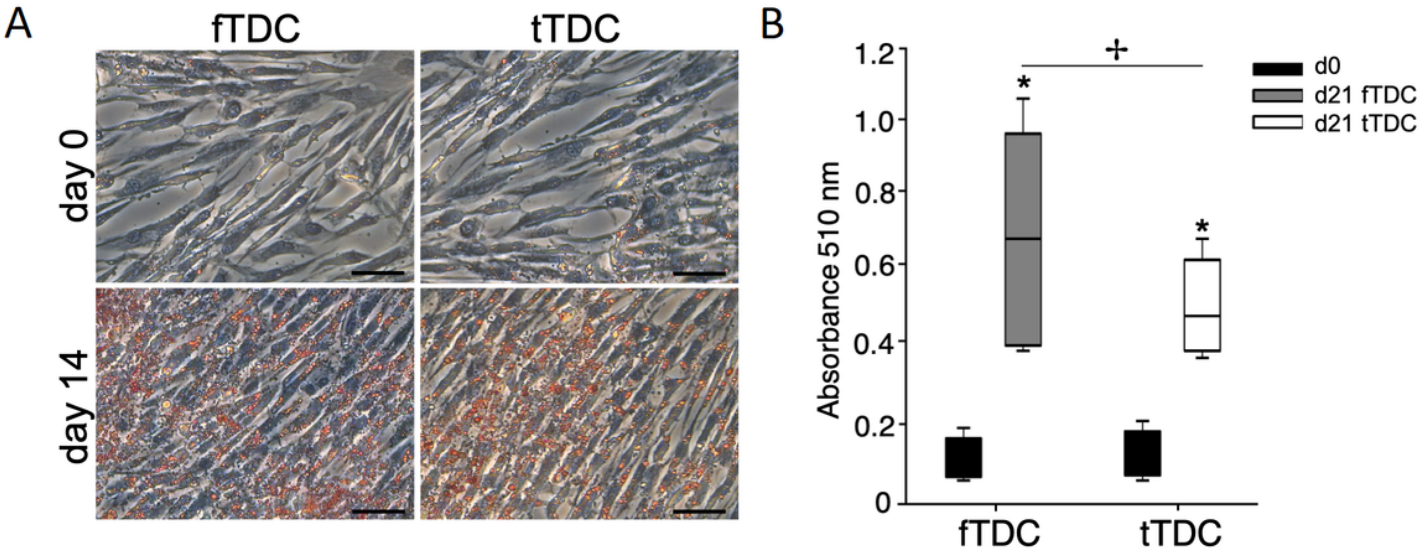

Figure 6

Adipogenesis of fTDC and tTDC. (a) Oil-Red-O staining of day 0 and 14 adipogenic cultures. Cytoplasmic lipid droplets were present in day 14 fTDC and tTDC; however, the cells retained their fibroblast morphology. Scale bar = 100 microns (b) Absorbance readings (mean + SD) following dye elution of Oil-

Red-O stained day 0 and 14 cultures. * represents significant difference ($P < 0.05$) from day 0 cultures. represents significant difference ($P < 0.05$) between day 14 fTDC and tTDC. n = 3.

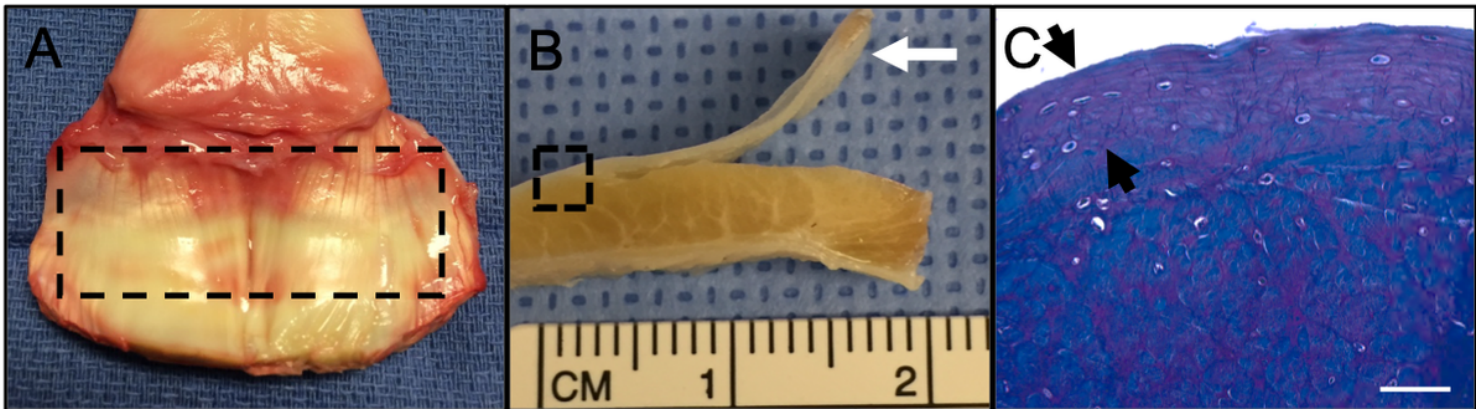

Figure 7

Equine intrasynovial DDFT structure and TDC isolation. (a) Equine forelimb intrasynovial DDFT within the hoof capsule. The outlined area (dashed line) represents tissue within the podotrochlear bursa that was used to isolate TDC. (b) Gross cross-section of DDFT with dorsal fibrocartilage dissected (arrow) from the underlying tendinous tissues. (c) Toluidine blue-stained cross section of DDFT (area outlined with a dashed line in B) that depicts chondrocyte-like cells within the proteoglycan-rich dorsal fibrocartilage (black arrow heads). Scale bar = 500 microns.

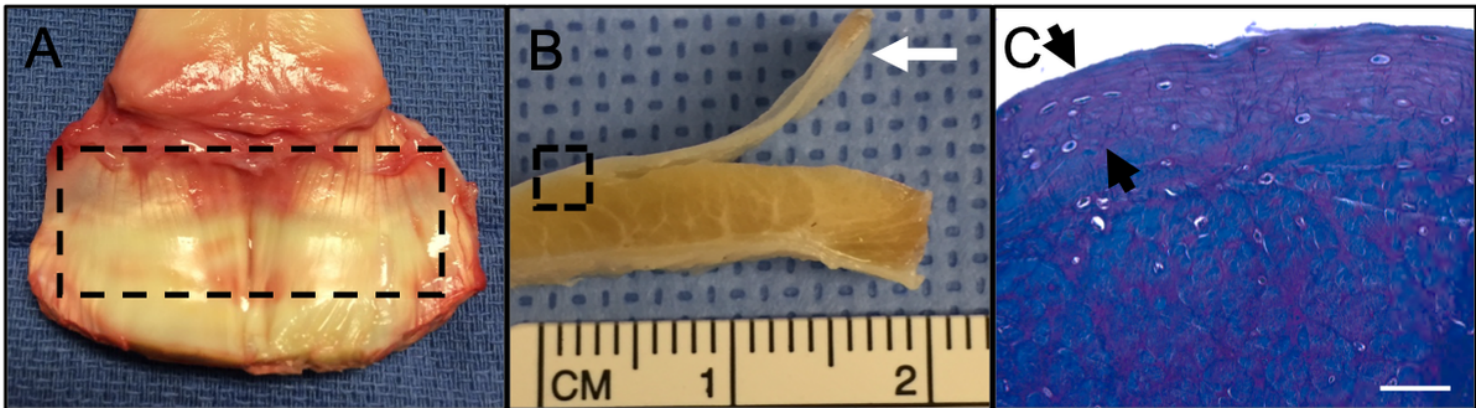

Figure 7

Equine intrasynovial DDFT structure and TDC isolation. (a) Equine forelimb intrasynovial DDFT within the hoof capsule. The outlined area (dashed line) represents tissue within the podotrochlear bursa that was used to isolate TDC. (b) Gross cross-section of DDFT with dorsal fibrocartilage dissected (arrow) from the underlying tendinous tissues. (c) Toluidine blue-stained cross section of DDFT (area outlined with a dashed line in B) that depicts chondrocyte-like cells within the proteoglycan-rich dorsal fibrocartilage (black arrow heads). Scale bar = 500 microns.